Coordination Structure of Adsorbed Zn(II) at Water-TiO_2 Interfaces

Guangzhi He[†], Gang Pan*[†], Meiyi Zhang[†], and Glenn A. Waychunas[‡]

[†]State Key Laboratory of Environmental Aquatic Chemistry, Research Center for Eco-Environmental Sciences, Chinese Academy of Sciences, Beijing 100085, China

[‡]Earth Sciences Division, Lawrence Berkeley National Laboratory, Berkeley, California 94720, United States

ABSTRACT: The local structure of aqueous metal ions on solid surfaces is central to understanding many chemical and biological processes in soil and aquatic environments. Here, the local coordination structure of hydrated Zn(II) at water-TiO_2 inter faces was identified by extended X-ray absorption fine structure (EXAFS) and X-ray absorption near-edge structure (XANES) spectroscopy combined with density functional theory (DFT) calculations. A nonintegral coordination number of average ~4.5 O atoms around a central Zn atom was obtained by EXAFS analy sis. DFT calculations indicated that this coordination structure was consistent with the mixture of 4-coordinated bidentate bi nuclear (BB) and 5-coordinated bidentate mononuclear (BM) metastable equilibrium adsorption (MEA) states. The BB com plex has 4-coordinated Zn, while the monodentate mononuclear (MM) complex has 6-coordinated Zn, and a 5-coordinated adsor bed Zn was found in the BM adsorption mode. DFT calculated energies showed that the lower-coordinated BB and BM modes were thermodynamically more favorable than the higher-coordinated MM MEA state. The experimentally observed XANES fingerprinting provided additional direct spectral evidence of 4-and 5 coordinated Zn-O modes. The overall spectral and computational evidence indicated that Zn(II) can occur in 4-, 5-, and 6-oxygen coordinated sites in different MEA states due to steric hindrance effects, and the coexistence of different MEA states formed the multiple coordination environments.

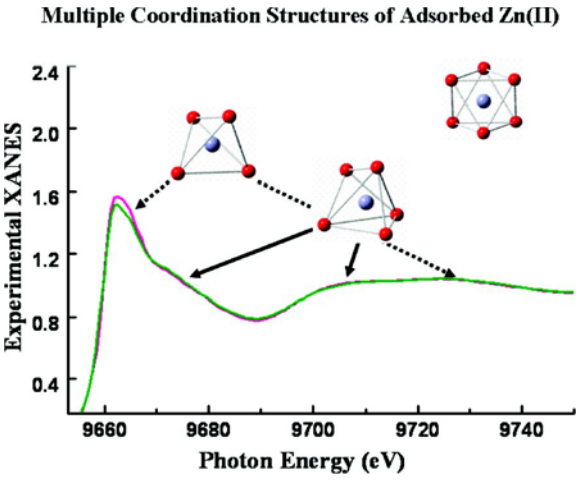

INTRODUCTION

The coordination behavior and interfacial structure of aqueous metal ions is a key issue in surface science and is subject to intense scrutiny and debate.[1-4].Differences in surface coordination structure may greatly affect the local chemical properties, long-range interactions, surface reactivity, and bioavailability of metal ions in the aquatic environment. For instance, the transformation of Zn coordination number from 6 to 4 during long-term incorporation into cells and short-term adsorption on diatom surfaces has been observed in the literature.[5] Such a change of metal local structure and/or species produces a significant isotopic fractionation of zinc between diatoms and Zn-bearing solution[6]. Conclusive diagnosis of the surface coordination structures of metal ions on the atomic scale is helpful for understanding the toxicity and environmental impacts of the pollutants.

Zinc is a ubiquitous metal ion in soil and aquatic environments and is of great environmental concern[7]. So far, although Zn(II) surface chemistry has been investigated extensively, there remains controversy as to its interfacial adsorption structures.[4,8,9] The current identification of the coordination structures of absorbed Zn has been based either on spectral and theoretical methods, such as extended X-ray absorption fine structure (EXAFS) and density functional theory (DFT) calculations[8,10–12] or on semiempirical hypotheses according to the variety of Zn coordination observed in crystalline compounds where Zn can occur in 4-, 5-, and 6-oxygen coordinated sites.[1,4,13] However, because the actual adsorption equilibrium state is generally constructed from a set of different microscopic metastable equilibrium adsorption (MEA) structures,[8,10,14] and the transformation/proportion among the MEA states can be affected by reaction kinetics,[7,15,16] the identification of separate MEA states in a given sample from EXAFS analysis is extremely difficult.[10,17] DFT calculations have been used to identify possible coordination environments of adsorbed Zn; these efforts demonstrated the influence of hydrolysis on adsorbate coordination number.[8] However, these DFT calculated results need to be confirmed from experimental evidence. Conclusive diagnosis and direct experimental evidence on the complex coordination

geometry of adsorbed Zn is lacking. This is partially due to the absence of high-sensitivity experimental techniques and theoretical analyses that can directly detect the local structure of adsorption states.

Synchrotron-based X-ray absorption near-edge structure (XANES) spectroscopy directly probes the unoccupied density of states (DOS) and gives three-dimensional stereochemical information on the electronic distribution and local geometry of the target atom.[15,17] The DOS function contains the individual contribution of atomic orbitals to a molecular orbital. The greater the DOS, the greater the probability of electron transition into a corresponding antibonding molecular orbital.[18] XANES is also very sensitive to valence changes and covalency, which allows XANES spectra to be potentially effective for distinguishing among different coordination structures. Therefore, the combination of high-accuracy EXAFS and XANES spectral analysis with DFT calculations is expected to provide substantial experimental and theoretical insights in the surface topology of metal ions on natural minerals [e.g., iron, aluminum, manganese, and titanium (hydr)oxides]. This effort may enable a more accurate identification of Zn surface coordination structures and thus allow enhanced understanding of the speciation and the geochemical cycle of zinc.

The objectives of this study were to determine the coordination properties of adsorbed Zn(II) and to provide new interpretation of the EXAFS analysis. For this purpose, the coordination microstructures of hydrated Zn(II) on TiO_2 surfaces obtained by EXAFS were further analyzed by DFT calculations, and the DFT-calculated interpretation of the nonintegral coordination numbers was directly confirmed by experimental XANES spectroscopy. TiO_2 was employed because it is a model oxide surface and widely used material in many interface-related studies including the treatment of various pollutants.[19−21]

THEORETICAL METHODS

Density Functional Theory Calculation. Calculations were performed via gradient-corrected density functional theory with the Becke three-parameter nonlocal exchange functional[22] and the Lee−Yang−Parr correlation functional[23] (i.e., B3LYP). Low-spin and restricted closed-shell formula with a fully optimized calculation strategy were employed to compute the adsorption of hydrated Zn(II) on titanium (hydr)oxide surfaces. To eliminate boundary effects and reduce charge on the clusters, the dangling bonds of O atoms were saturated with H atoms.[16,24,25] The geometry and energy were calculated by use of the 6-31G(d) basis set for O and H and the LANL2DZ relativistic effective core potential basis set for Zn and Ti transition metals.

Because of the high computational cost of electronic structure methods, a Ti_4O_{18} cluster representing the (100) anatase surface was used to determine the geometry of Zn(II)−TiO_2 complexes. The surfaces of anatase particles consist predominantly of (101), (100), and (001) crystal planes,[26,27] with the specific expression of crystal planes (i.e., the crystal habit) depending on the synthesis technique.[28,29] Our previous studies proved that the dominant surface in the TiO_2 powder used in our adsorption experiments was the (100).[15,16] The good agreement of calculated Zn−O and Zn−Ti distances with experimental EXAFS results also indicated the reliability and agreement between the crystal planes and model cluster used in our calculations.

There are two different oxygen sites in anatase, O(2) and O(3), which are bonded by two and three titanium atoms, respectively.[29] The 16 boundary oxygens in the Ti_4O_{18} model cluster were saturated with 22 H atoms to ensure the coordination numbers of O(2) and O(3) were the same as that of anatase bulk structure. This method avoided the overrelaxation of model clusters[16,30] (discussed in the Supporting Information). Six water molecules were used to simulate the hydration of the Zn(II) cation. Therefore, a $[Ti_4O_2(OH)_{10}(H_2O)_6Zn(H_2O)_6]^{4+}$ cluster model was ultimately used to determine the geometry of Zn(II)−TiO_2 adsorption states. This cluster model was verified to be reliable to describe the typical adsorption sites of Zn(II) and identify the coordination properties of Zn(II)−TiO_2 complex (discussed in the Supporting Information). The DFT calculation was performed with Gaussian03.[31]

X-ray Absorption Near-Edge Structure Simulation. Zn K-edge XANES spectra and projected density of states were calculated by full multiple scattering theory (i.e., all scattering paths were summed within a specified cluster volume) by use of a self-consistent field potential model with the FEFF 8.2 code.[32] The self-consistent field potential model is more accurate for XANES calculation than atomic overlap using the Mattheiss prescription, because the former takes the charge transfer into account and is more reliable in estimating the Fermi level E_F.[15,33] In the calculation, the Hedin−Lundqvist exchange−correlation potential was used with muffin-tin radii overlap of 0.8 for H atom and 1.15 for other atoms (i.e., Zn, O, and Ti atoms).[33] A core hole was included to imitate the final state of the photon absorption process. Each type of scatterer (i.e., O, H, and Ti atoms) was calculated with unique potentials.[17] The XANES simulation was on the basis of a ∼8.0 Å radius Zn(II)−TiO_2 surface adsorption cluster (typically ∼140 atoms), in which convergence had occurred. In the XANES model clusters (presented in the Supporting Information), the geometries of zinc and the first-neighbor oxygen atoms were optimized via a DFT calculation, while the substrate used the bulk structure of the anatase (100) surfaces.

EXPERIMENTAL SECTION

Materials and Sample Preparation. Zinc stock solution was prepared from $Zn(NO_3)_2$ (guaranteed reagent, Beijing Chemical Reagents Co.) and stored at 4 °C. Other reagents used in this study were analytical-grade, and all labware was acid-washed. Anatase TiO_2 (Beijing Chemical Reagents Co.) was used as the adsorbent. X-ray diffraction analyses showed that the TiO_2 was pure anatase. Brunauer−Emmett−Teller (BET) surface area analysis (ASAP-2010, Micromeritics) following the standard N_2−BET method indicated a specific surface area of 201.3 m^2/g for the dry TiO_2. Because of the aggregation effect, the particle size distribution in solution, measured with a Mastersizer 2000 analyzer (Malvern), ranged from 0.3 to 2.5 μm. The volume average particle diameter was 0.95 μm. All solutions were prepared in ultrapure water (resistivity 18 MΩ) obtained with a Liyuan UPW-10N ultrapure water system.

To study the interfacial structures of hydrated Zn(II) on TiO_2 surfaces, adsorption samples were prepared at pH 6.3 and 6.8 for XAFS measurement. The two samples were chosen from the pH edge of Zn(II) on anatase[34] and generated by adding different total zinc concentration (0.41 mmol/L for pH 6.3 and 0.77 mmol/L for pH 6.8) to polypropylene centrifuge tubes with 1.0 g/L TiO_2, and 30 mL volume, to yield sufficient adsorption density for XAFS data collection. A constant ionic strength was maintained by use of 0.01 mol/L $NaNO_3$. The pH of the reaction

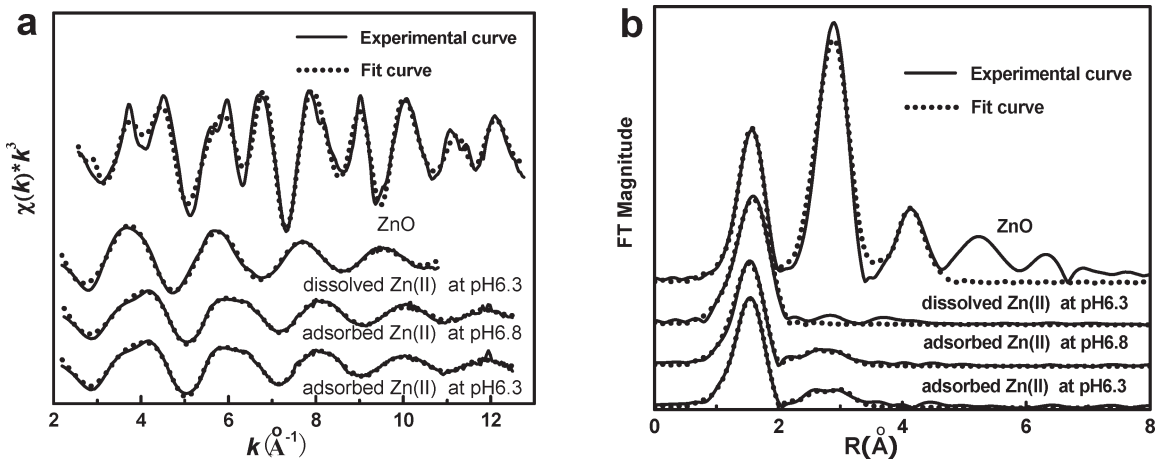

Figure 1. (a) k^3-weighted observed (—) and fitted (---) Zn K-edge EXAFS spectra of adsorption samples and reference materials. (b) Zinc RSFs (radial structural functions) for adsorption samples and reference materials. The peak positions are uncorrected for phase shifts.

system was constantly monitored and adjusted to the desired value (6.3 and 6.8) by addition of 0.1 mol/L NaOH or 0.1 mol/L HNO_3. The tubes were capped and shaken for 24 h at 25 °C, during which the adsorption reached equilibrium. After 24 h of equilibration, the moist Zn-laden TiO_2 solids were separated by centrifugation and mounted in 2 mm thick sample holders. The samples were sealed between two layers of adhesive poly(vinyl chloride) (PVC) tape to prevent moisture loss and stored at 4 °C before XAFS measurement.

X-ray Absorption Fine Structure Measurement and Data Treatment. XAFS data were measured on beamline 4W1B at the Beijing Synchrotron Radiation Facility (BSRF). A spectral range of −120 to 1100 eV from the K-absorption edge of Zn (9659 eV) was collected under ambient conditions. Si(111) monochromator crystals (allowing energy resolution of 0.5 eV at the Zn K-edge) were utilized. The XAFS spectra of adsorption samples were collected with a Lytle ionization detector in fluorescence mode due to the relatively low Zn concentration (0.27 mmol/g for pH 6.3 and 0.62 mmol/g for pH 6.8). The reference materials, ZnO powder and zinc aqueous solutions (0.1 mol/L), were measured in the transmission mode. The fluorescence signal was filtered by a Cu foil and radial Soller slit assembly to reduce the elastically scattered radiation. An average of three scans was performed to achieve an adequate signal/noise ratio. The energy of the Zn K-absorption edge (9659 eV) was calibrated with Zn foil.

The XAFS data were processed following the standard procedures of background absorption removal, normalization, conversion to k-space, and Fourier transformation, and then the EXAFS geometric information was extracted by use of the WinXAS 3.1 software package[1,16,35] with Fourier filtering and shell fitting. A linear function fit for the pre-edge region and a second-order polynomial fit in the post-edge region were used for normalization to remove the background absorption. The experimental XANES analysis utilized the background-corrected and normalized spectra obtained at this point.

Subsequently for EXAFS analysis, normalized spectra were converted to frequency (k) space by use of a cubic spline, weighted by k^3, and weighted $k^3\chi(k)$ spectra were generated. The $k^3\chi(k)$ spectra, from 2.2 to 12.5 Å^{-1}, were Fourier-transformed (FT) by use of a Bessel window function with smoothing parameter of 4 to produce the radial structure function (RSF) in R-space (angstroms). The structural parameters of adsorption samples and zinc solution reference were determined by fitting theoretical phase-shift and amplitude functions of Zn−O and Zn−Ti scattering paths calculated by ab initio FEFF 8.2 code for the cluster of zinc titanate (Zn_2TiO_4). The body amplitude reduction factor (S_0^2) of 0.87 was used for data fitting.[4,12] The ZnO reference was fitted by use of the Zn−O and Zn−Zn scattering paths calculated from the crystalline structure of ZnO to estimate the accuracies for the fit parameters. All fits were performed in a sequential manner, by adding backscattering paths stepwise and recording reductions of the residual of the fit. Shells were added in order of distance from the central target atom. The coordination number (CN) of Zn−O shell and two Zn−Ti shells were initially fixed at 4, 1, and 2, respectively, to obtain estimated values for interatomic distances (R) and Debye−Waller factors σ^2. Then the interatomic distances (R) and σ^2 were fixed to obtain CN and ΔE_0 (within ±7.0 eV) for each shell. The estimated values of CN, R, σ^2, and ΔE_0 were then used for a sequential fitting that recorded the reduction of the residual until the best fit was obtained. All the parameters (CN, R, σ^2, and ΔE_0) for each backscattering path were allowed to vary progressively in the fitting processes. Residual was less than 6%, indicating the high quality of the final data fitting. To confirm the EXAFS fitting results, the experimental spectra were also fitted by use of the DFT-calculated adsorption complexes as fitting models with the same EXAFS procedures described above (detailed data are presented in the Supporting Information).

RESULTS AND DISCUSSION

Extended X-ray Absorption Fine Structure Analysis. The k^3-weighted and Fourier transform spectra of Zn K-edge EXAFS for reference materials and adsorption samples at pH 6.3 and 6.8 are given in Figure 1. Structural parameters of EXAFS fitting are presented in Table 1. The comparison of our fit results for ZnO reference with the standard values[36] indicated that the estimated accuracies of the first coordination shell were ±3% for CN and ±0.01 Å for R. Our fitting results show that the first coordination shell of the adsorbed Zn consisted of ~4.5 oxygen atoms at a distance of ~2.00 Å, suggesting a multiple coordination environment. This result agrees with the fitting using the DFT-calculated adsorption models (discussed in the Supporting Information). This coordination situation of Zn(II) has been commonly observed in the literature and has been attributed either to

Table 1. EXAFS Measured Structural Parameters of Zn(II) Adsorption on Titanium (Hydr)oxides[a]

	Zn−O			Zn−Ti subshell 1			Zn−Ti subshell 2			
sample	CN	R (Å)	σ^2	CN_1	R_1 (Å)	σ^2	CN_2	R_2 (Å)	σ^2	residual
adsorbed Zn(II), pH 6.3	4.4	1.99	0.007	1.0	3.18	0.007	1.9	3.40	0.01	5.3
adsorbed Zn(II), pH 6.8	4.5	2.00	0.008	1.1	3.16	0.01	1.7	3.43	0.01	5.6
dissolved Zn(II), pH 6.3	6.1	2.07	0.009							2.5
ZnO	4.1	1.97	0.004							9.0

[a] Progressive reduction of the residual was recorded for each additional shell added to the fit. The listed parameters (CN, coordination number; R, interatomic distance; σ^2, Debye−Waller factor) reflect the final best fit.

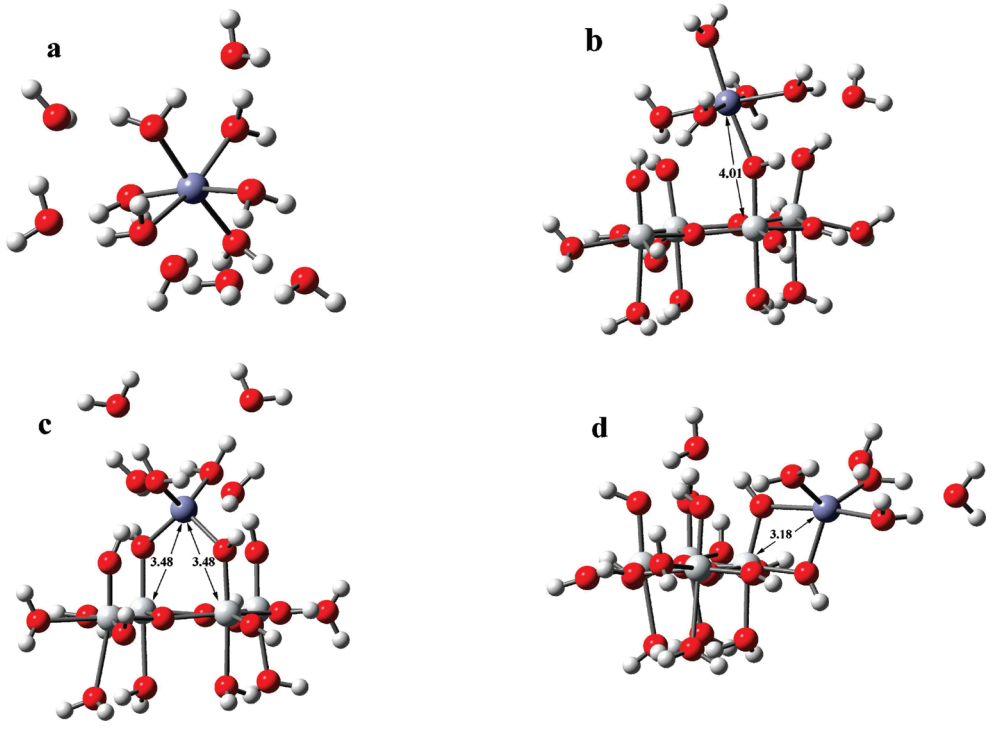

Figure 2. Calculated Zn(II)−TiO_2 surface complexes from density functional theory: (a) dissolved Zn(II) with six outer-sphere water molecules; (b) monodentate mononuclear (MM); (c) bidentate binuclear (BB); (d) bidentate mononuclear (BM). Purple, red, large gray, and small gray circles denote Zn, O, Ti, and H atoms, respectively. Distances are shown in angstroms.

distortion in the first coordination shell or to a mixture of tetrahedral (4-oxygen coordinated) and octahedral (6-oxygen coordinated) sites.[1,7,10,11,37]

Density Functional Theory Calculation. For Zn(II) (pK_{a1} = 8.2−9.0), the $Zn(H_2O)_6^{2+}$ hydration state is the dominant species at pH 6.3 and 6.8.[8,38] On the basis of the acid dissociation constants of TiO_2 surfaces (pK_{a1} = 3.8, pK_{a2} = 7.8),[16,21] ≡TiOH surface is the dominant surface functional group of TiO_2 in the experimental pH range from 6.3 to 6.8. Thus, the $Zn(H_2O)_6^{2+}$ hydration state and a singly hydroxylated TiO_2 surface (i.e., ≡TiOH surface) was used in the DFT calculation. The DFT-calculated structures for corner-sharing and edge-sharing Zn with the TiO_2 surfaces are shown in Figure 2.

DFT results indicated that the dissolved Zn(II) stably existed in a 6-oxygen coordinated octahedron in solution, and the first shell of Zn was occupied by either four, five, or six O atoms in different adsorption states due to the interferences created by steric hindrance (Figure 2). The DFT calculation showed that the first shell of Zn was occupied by four O atoms for bidentate binuclear (BB) complex, five O atoms for bidentate mononuclear (BM) complex, and six O atoms for monodentate mononuclear (MM) complex (Figure 2). Due to the repulsion of inner-sphere water molecules, the mean Zn−O distance increased from 2.01 to 2.14 Å as the coordinated O atoms increased from 4 to 6 (Table 2).

Table 2. DFT Calculated Structural Parameters and Relative Energies of Zn(II)−TiO_2 Adsorption Complexes

	Zn−O		Zn−Ti		
calcd values	CN	R (Å)	CN	R (Å)	relative energy (kcal/mol)
dissolved Zn(II)	6.0	2.13			
MM	6.0	2.14	1	4.01	0.00
BB	4.0	2.01	2	3.48	−8.58
BM	5.0	2.07	1	3.18	−15.15

EXAFS analysis results showed that the second coordination shell of the Zn(II)−TiO_2 surface complexes was dominated by

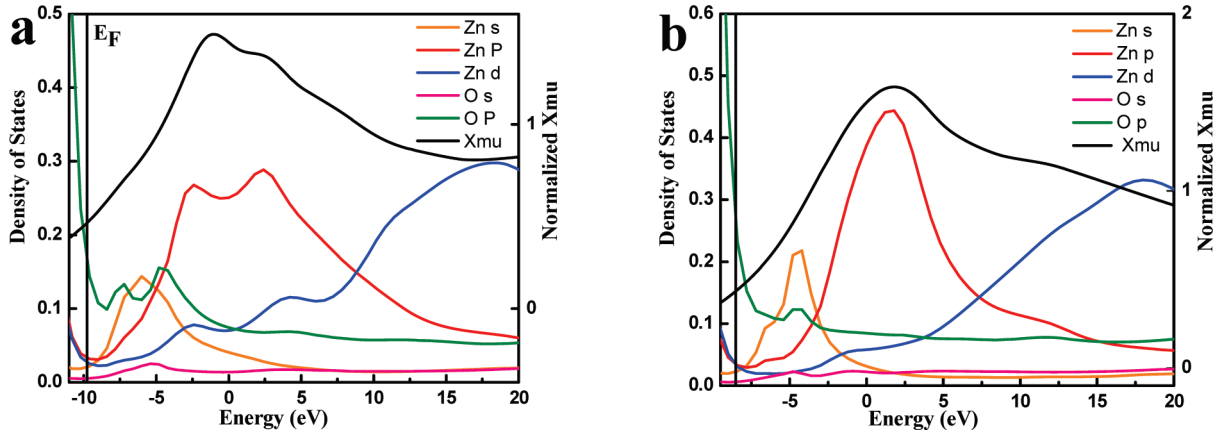

Figure 3. Projected density of states and calculated XANES spectra: (a) BB complex; (b) BM complex.

two titanium subshells at Zn−Ti distances of ∼3.17 and ∼3.42 Å (Table1). The two experimental Zn−Ti distances were close to the DFT calculated values of BM edge-sharing (3.18 Å) and BB corner-sharing (3.48 Å) complexes (Table 2 and Figure 2c,d). In the MM corner-sharing mode, Zn would be coordinated by six O atoms at ∼2.14 Å and yield a Zn−Ti distance near 4.00 Å (Table 2 and Figure 2b), both much larger than the distances obtained from EXAFS analysis (Table 1). DFT calculated energies showed that the 6-oxygen coordinated MM complex was an energetically unstable metastable equilibrium adsorption (MEA) state compared with the BB (−8.58 kcal/mol) and BM (−15.15 kcal/mol) adsorption modes (Table 2). Zn(II) is bonded to TiO_2 surfaces by only one chemical bond in the monodentate linkage mode but by two bonds in the bidentate mode (Figure 2). Hence, the Zn−O bonding interaction and the topological stabilization are enhanced by the high electron density between Zn and O in the BB and BM adsorption geometries, compared to the MM MEA state. This evidence indicated that the MM linkage mode would be minor in the adsorption of Zn(II) on TiO_2 under the conditions we examined. The MM adsorption mode was therefore excluded in the XANES analysis we described below.

DFT-calculated Zn−O distances for both dissolved and adsorbed Zn complexation models were generally longer than the experimentally measured values. This difference between experimental and theoretical values has been attributed to the theoretical underestimation of solvent effect from outer-sphere water molecules.[39] However, we expect that this artifact does not affect the relative stability of the adsorption modes and their coordination properties.

X-ray Absorption Near-Edge Structure Analysis. *Density of States Analysis.* The projected density of states and calculated XANES spectra of 4-coordinated BB and 5-coordinated BM Zn(II)−TiO_2 surface complexes are presented in Figure 3. The occupied molecular orbitals were those below the Fermi level E_F, and the antibonding molecular orbitals were those above E_F.[15,33] Comparison between the absorption edge position and valence orbital density (Figure 3) indicated that the XANES absorption edge was primarily due to the dipole transition from Zn 1s electron into the Zn(3p)−O(2p) antibonding molecular orbital. The results of density of states showed that the degeneracy of the Zn(3p) orbital (Figure 3a) occurred in the symmetrical 4-coordinated BB complex (Figure 3b, belongs to C_{2v} point group), which leads to an electronic doublet transition from the Zn 1s

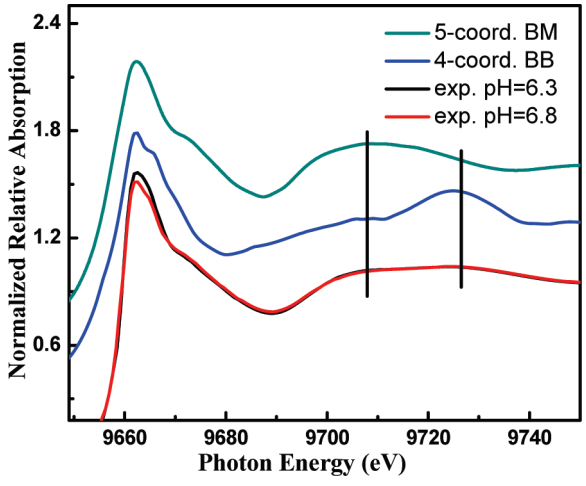

Figure 4. Calculated XANES spectra of 4-oxygen coordinated BB and 5-oxygen coordinated BM complex and experimental XANES spectra.

atomic orbital into the Zn(3p)−O(2p) antibonding molecular orbitals and forms a shoulder above the energy of the Zn K-edge (Figure3a). Different from the 4-oxygen coordinated BB complex, the high density of the Zn(3d) orbital and hence the greater transition probability from the Zn 1s electron into the Zn-(3d)−O(2p) antibonding molecular orbital occurs for the 5-oxygen coordination Zn polyhedron, which results in an absorption oscillation in the BM complex at an energy position of ∼10.0 eV higher than the absorption edge (Figure 3b). These results indicated that the density of states and low-energy XANES (from pre-edge up to ∼10 eV beyond the absorption edge) was an effective probe for the coordination geometry around the target atom. We found that none of the occupied states (e.g., core electrons, Ti−O and Zn−O bonding orbitals, oxygen lone pairs) directly contributed to XANES spectra.

Theoretical Analysis of Experimental XANES. Experimental and calculated XANES spectra are presented in Figure 4. There was no obvious difference in experimental XANES between the two samples (Figure 4), suggesting a stable inner-sphere spatial population and complexation of Zn(II) on TiO_2 surfaces under the pH condition from 6.3 to 6.8, which was in accordance with the EXAFS- measured structural results (Table 1). The theoretical XANES spectra of BB and BM complexes reproduced all absorption characteristics (absorption edge, post-edge absorption

oscillation and shape resonances) from the experimental XANES spectra (Figure 4), indicating they they were appropriate for a description fo the real complexation of Zn(11) on TiO2 surfaces

Different from the low-energy XANES (from pre-edge up to ~10 eV beyond the absorption edge) that is primarily dominated by the electronic structure encompassing the target atom, high-energy XANES (from post-edge ~10 eV up to ~50 eV beyond the absorption edge) results from the single and multiple scattering effects from the neighbor atoms around the target atom. Several shape resonances that directly reproduce the distribution of the neighbor coordination atoms may be formed in the high-energy XANES area.[32] The experimentally measured two post-edge shape resonances agreed with the theoretical absorption of 5-coordinated BM (at 9708.0 eV) and 4-coordinated BB surface complex (at 9725.0 eV), respectively (Figure 4).

All the XANES evidence suggests that the BB and BM complexation modes coexisted in one sample and have distinct coordination structures, a finding consistent with the EXAFS and DFT results. Because the arrangement of atoms array in the real system is not as ideal as that of the calculated cluster model, the disorder of the real system leads to the broadening and weakening of the characteristic absorption in experimental XANES (Figure 4).[17,33]

The overall spectral and computational evidence indicated that the coordination complexity of Zn(II) cation was due to the fact that each metastable equilibrium adsorption (MEA) state has a unique inner-sphere O coordinated site. The coexistence of different MEA states formed the multiple coordination environments.

Environmental Implications. This study provided a new interpretation of the EXAFS data by use of DFT calculations and experimental XANES analysis for metal ion adsorption on oxide surfaces. The coordination complexity of adsorbed Zn(II) suggested a potential new development of surface complexation models that can take into account the microscopic coordination structures in describing the macroscopic relationship between equilibrium concentrations in solution and on solid surfaces. The atomic-level identification of surface coordination geometry helps improve our understanding of the toxicity and environmental impacts of metal ions, because the change of metal coordination structure may produce a significant impact on its speciation and transport in the environment.

ACKNOWLEDGMENT

The study was supported by NNSF of China (20777090, 21007083, 20921063). We thank the Beijing Synchrotron Radiation Facility (BSRF, China) for providing the beam time and Shuang Gao, Tiandou Hu, Ziyu Wu, and Yaning Xie for valuable assistance in XAFS experiment. G.A.W. is supported by the Office of Basic Energy Sciences, Chemical Sciences, Geosciences, and Biosciences Division of the U.S. Department of Energy under Contract DE-AC02-05CH11231.

REFERENCES

(1) Grafe, M.; Sparks, D. L. Kinetics of zinc and arsenate co-sorption at the goethite-water interface. Geochim. Cosmochim. Acta 2005, 69 (19), 4573–4595.

(2) Lee, S. W.; Anderson, P. R. EXAFS study of Zn sorption mechanisms on hydrous ferric oxide over extended reaction time. J. Colloid Interface Sci. 2005, 286 (1), 82–89.

(3) Sverjensky, D. A. Physical surface-complexation models for sorption at the mineral-water interface. Nature 1993, 364 (6440), 776–780.

(4) Waychunas, G. A.; Fuller, C. C.; Davis, J. A. Surface complexation and precipitate geometry for aqueous Zn(II) sorption on ferrihydrite I: X-ray absorption extended fine structure spectroscopy analysis. Geochim. Cosmochim. Acta 2002, 66 (7), 1119–1137.

(5) Pokrovsky, O. S.; Pokrovski, G. S.; Gelabert, A.; Schott, J.; Boudou, A. Speciation of Zn associated with diatoms using X-ray absorption spectroscopy. Environ. Sci. Technol. 2005, 39 (12), 4490– 4498.

(6) Gelabert, A.; Pokrovsky, O. S.; Pokrovski, G. S.; Viers, J.; Schott, J.; Boudou, A. Zinc interaction with diatom cultures: New insights from XAFS study and stable isotope fractionation. Geochim. Cosmochim. Acta 2004, 68 (11), A366–A366.

(7) Roberts, D. R.; Ford, R. G.; Sparks, D. L. Kinetics and mechanisms of Zn complexation on metal oxides using EXAFS spectroscopy. J. Colloid Interface Sci. 2003, 263 (2), 364–376.

(8) Zhang, Z.; et al. Structure of hydrated $Zn^{2þ}$ at the rutile TiO2 (110)-aqueous solution interface: Comparison of X-ray standing wave, X-ray absorption spectroscopy, and density functional theory results. Geochim. Cosmochim. Acta 2006, 70 (16), 4039–4056.

(9) Schlegel, M. L.; Manceau, A. Zn incorporation in hydroxy-Aland Keggin Al-13-intercalated montmorillonite: A powder and polarized EXAFS study. Environ. Sci. Technol. 2007, 41 (6), 1942–1948.

(10) Ha, J. Y.; Trainor, T. P.; Farges, F.; Brown, G. E. Interaction of aqueous Zn(II) with hematite nanoparticles and microparticles. Part 1. EXAFS study of Zn(II) adsorption and precipitation. Langmuir 2009, 25 (10), 5574–5585.

(11) Lee, S.; Anderson, P. R.; Bunker, G. B.; Karanfil, C. EXAFS study of Zn sorption mechanisms on montmorillonite. Environ. Sci. Technol. 2004, 38 (20), 5426–5432.

(12) Li, W.; Pan, G.; Zhang, M. Y.; Zhao, D. Y.; Yang, Y. H.; Chen, H.; He, G. Z. EXAFS studies on adsorption irreversibility of Zn(II) on TiO2: Temperature dependence. J. Colloid Interface Sci. 2008, 319 (2), 385–391.

(13) Manceau, A.; Marcus, M. A.; Tamura, N.; Proux, O.; Geoffroy, N.; Lanson, B. Natural speciation of Zn at the micrometer scale in a clayey soil using X-ray fluorescence, absorption, and diffraction. Geochim. Cosmochim. Acta 2004, 68 (11), 2467–2483.

(14) Pan, G.; Qin, Y. W.; Li, X. L.; Hu, T. D.; Wu, Z. Y.; Xie, Y. N. EXAFS studies on adsorption-desorption reversibility at manganese oxides-water interfaces I. Irreversible adsorption of zinc onto manganite (gamma-MnOOH). J. Colloid Interface Sci. 2004, 271 (1), 28–34.

(15) He, G. Z.; Pan, G.; Zhang, M. Y.; Wu, Z. Y. Quantitative XANES studies on metastable equilibrium adsorption of arsenate on TiO2 surfaces. J. Phys. Chem. C 2009, 113 (39), 17076–17081.

(16) He, G. Z.; Zhang, M. Y.; Pan, G. Influence of pH on initial concentration effect of arsenate adsorption on TiO2 surfaces: thermodynamic, DFT and EXAFS interpretations. J. Phys. Chem. C 2009, 113, 21679–21686.
(17) Waychunas, G. A.; Fuller, C. C.; Davis, J. A.; Rehr, J. J. Surface complexation and precipitate geometry for aqueous Zn(II) sorption on ferrihydrite: II. XANES analysis and simulation. Geochim. Cosmochim. Acta 2003, 67 (5), 1031–1043.
(18) Khare, N.; Martin, J. D.; Hesterberg, D. Phosphate bonding configuration on ferrihydrite based on molecular orbital calculations and XANES fingerprinting. Geochim. Cosmochim. Acta 2007, 71 (18), 4405– 4415.
(19) Malato, S.; Caceres, J.; Aguera, A.; Mezcua, M.; Hernando, D.; Vial, J.; Fernandez-Alba, A. R. Degradation of imidacloprid in water by photo-fenton and TiO_2 photocatalysis at a solar pilot plant: A comparative study. Environ. Sci. Technol. 2001, 35 (21), 4359–4366.
(20) Vinu, R.; Madras, G. Kinetics of sonophotocatalytic degradation of anionic dyes with nano-TiO2. Environ. Sci. Technol. 2009, 43 (2), 473–479.
(21) Pena, M.; Meng, X. G.; Korfiatis, G. P.; Jing, C. Y. Adsorption mechanism of arsenic on nanocrystalline titanium dioxide. Environ. Sci. Technol. 2006, 40 (4), 1257–1262.
(22) Becke, A. D. Density-functional thermochemistry. 3. The role of exact exchange. J. Chem. Phys. 1993, 98 (7), 5648–5652.
(23) Lee, C. T.; Yang, W. T.; Parr, R. G. Development of the Colle-Salvetti correlation-energy formula into a functional of the electron-density. Phys. Rev. B 1988, 37 (2), 785–789.
(24) Paul, K. W.; Kubicki, J. D.; Sparks, D. L. Quantum chemical calculations of sulfate adsorption at the Al- and Fe-(Hydr)oxide-H_2O interface—Estimation of Gibbs free energies. Environ. Sci. Technol. 2006, 40 (24), 7717–7724.
(25) Sherman, D. M.; Randall, S. R. Surface complexation of arsenie
(V) to iron(III) (hydr)oxides: Structural mechanism from ab initio molecular geometries and EXAFS spectroscopy. Geochim. Cosmochim. Acta 2003, 67 (22), 4223–4230.
(26) Lazzeri, M.; Vittadini, A.; Selloni, A. Structure and energetics of stoichiometric TiO_2 anatase surfaces. Phys. Rev. B 2001, 63 (15), No. 155409.
(27) Vittadini, A.; Selloni, A.; Rotzinger, F. P.; Gratzel, M. Structure and energetics of water adsorbed at TiO_2 anatase (101) and (001) surfaces. Phys. Rev. Lett. 1998, 81 (14), 2954–2957.
(28) Beltran, A.; Sambrano, J. R.; Calatayud, M.; Sensato, F. R.; Andres, J. Static simulation of bulk and selected surfaces of anatase TiO_2. Surf. Sci. 2001, 490 (1-2), 116–124.
(29) Homann, T.; Bredow, T.; Jug, K. Adsorption of small molecules on the anatase (100) surface. Surf. Sci. 2004, 555 (1-3), 135–144.
(30) Hu, Z.; Turner, C. H. Atomic layer deposition of TiO2 from TiI_4 and H_2O onto SiO_2 surfaces: Ab initio calculations of the initial reaction mechanisms. J. Am. Chem. Soc. 2007, 129 (13), 3863–3878.
(31) Frisch, M. J., et al. Gaussian03, revision C.01wis2; Gaussian, Inc., Wallingford, CT, 2004.
(32) Ankudinov, A. L.; Ravel, B.; Rehr, J. J.; Conradson, S. D. Real-space multiple-scattering calculation and interpretation of X-ray-absorption near-edge structure. Phys. Rev. B 1998, 58 (12), 7565–7576.
(33) Ankudinov, A. L., et al. FEFF8, version 8.20; The FEFF Project, Department of Physics, University of Washington, 2002.
(34) Gao, S.; Chen, H.; He, G. Z.; Pan, G. EXAFS Studies of pH Effects on Adsorption and Microscopic Strutures of Zn(II) onto TiO_2. Chem. J. Chin. Univ.-Chin. 2009, 30 (12), 2439–2444.
(35) Ressler, T. WinXAS: a program for X-ray absorption spectroscopy data analysis under MS-Windows. J. Synchrotron Radiat. 1998, 5 (2), 118–122.
(36) Kihara, K.; Donnay, G. Anharmonic thermal vibrations in ZnO. Can. Mineral 1985, 23, 647–654.
(37) Trainor, T. P.; Brown, G. E.; Parks, G. A. Adsorption and precipitation of aqueous Zn(II) on alumina powders. J. Colloid Interface Sci. 2000, 231 (2), 359–372.
(38) Marcus, Y. A simple empirical-model describing the thermodynamics of hydration of ions of widely varying charges, sizes, and shapes. Biophys. Chem. 1994, 51 (2-3), 111–127.
(39) Zhu, M. Q.; Pan, G. Quantum chemical studies of mononuclear zinc species of hydration and hydrolysis. J. Phys. Chem. A 2005, 109 (33), 7648–7652.